## ON-LINE APPENDIX

### A) Murray's Optimality Principle

According to an elegant argument put forward by Murray in 1926,[1] the pumping power required to overcome frictional resistance of blood flowing through a vessel must be balanced by the metabolic power required to maintain the blood volume. Under the assumption of Poiseuille flow (fully developed, steady flow of a constant-viscosity fluid in a long, straight tube of circular cross-section), the pumping power is given by

$$P_{\text{pump}} = \frac{128\mu L Q^2}{\pi D^4}, \tag{A.1}$$

where $D$ is the vessel diameter, $L$ is the vessel length, $Q$ is the blood flow rate, and $\mu$ is the blood viscosity. The metabolic power required to maintain the (cylindric) volume of blood is given by

$$P_{\text{metab}} = kL\frac{\pi D^2}{4}, \tag{A.2}$$

where $k$ is an unknown-but-constant property of the blood. Mathematically, optimality is found when the derivative of the total power with respect to diameter is zero:

$$\frac{d(P_{\text{pump}} + P_{\text{metab}})}{dD} = -\frac{512\mu L Q^2}{\pi D^5} + kL\frac{\pi D}{2} = 0. \tag{A.3}$$

Noting that $Q$ and $D$ are properties of the vessel ($L$ cancels out), whereas $k$ and $\mu$ are (nominally constant) properties of the blood, Equation A.3 simplifies to

$$Q \propto D^3. \tag{A.4}$$

This is the basis for the so-called "cube law" or Murray's law, which has since been generalized to a power law:

$$Q \propto D^n, \tag{A.5}$$

where the value of $n$ may be closer to 2 in large conduit arteries, where the Poiseuille flow assumption no longer holds.[2]

### B) Murray's Law for a Simple Bifurcation

Considering now the case of a single vascular bifurcation having parent artery diameter $D_0$ and daughter branch diameters $D_1$ and $D_2$, it follows from Equation A.5 that the division of flow to the daughter branches should be

$$\frac{Q_2}{Q_1} = \left(\frac{D_2}{D_1}\right)^n. \tag{B.1}$$

Following Chnafa et al,[3] we refer to this as the "flow ratio" power law relation because it makes no assumption about the parent artery diameter. If one invoked conservation of flow

$$Q_0 = Q_1 + Q_2, \tag{B.2}$$

it follows that

$$D_0^n = D_1^n + D_2^n, \tag{B.3}$$

which, again following Chnafa et al,[3] we refer to as the "geometric" power law relation because it relates parent and daughter branch diameters. Equations B.1 and B.3 reduce to the standard Murray's law for a bifurcation when $n = 3$.

### C) Zero-Pressure Outflow for a Simple Bifurcation

Consider the simple bifurcation described above. If we prescribe the same pressure at both outlets, it follows that the pressure drop across both daughter branches must be the same because they originate at the same point, ie,

$$p_b - p_{\text{out}} = Q_1 R_1 \tag{C.1a}$$

$$p_b - p_{\text{out}} = Q_2 R_2, \tag{C.1b}$$

where $p_b$ is the (unknown) pressure at the bifurcation point, $p_{\text{out}}$ is the (prescribed) pressure at the outlets, and $R_i$ is the viscous flow resistance of branch $i$. It follows, simply, that

$$\frac{Q_2}{Q_1} = \frac{R_1}{R_2}. \tag{C.2}$$

Note that the flow division does not depend on the value of $p_{\text{out}}$, only that it is the same at both outlets. If, for the sake of argument, we assume Poiseuille flow in the branch—the same assumption underpinning Murray's Law—the branch flow resistance is given by

$$R_i = \frac{128\mu L_i}{\pi D_i^4}. \tag{C.3}$$

Substituting this into Equation C.2, we get

$$\frac{Q_2}{Q_1} = \frac{L_1 D_2^4}{L_2 D_1^4}. \tag{C.4}$$

In other words, for the zero-pressure method, the flow division will depend on both the relative diameters and the lengths of the outflow branches (as well as on the true nature of flow inside the branch, which, of course, is only known after the CFD simulation). In cerebrovascular CFD models, outlet lengths are usually ad hoc, driven by image quality, the presence of downstream branches, or operator preference. On the other hand, to facilitate the imposition of outflow conditions, cylindrical outflow extensions are often added to the CFD models. If these are sufficiently long and made proportional to the outlet diameter, ie,

$$L_i = kD_i, \tag{C.5}$$

the outflow division reduces to

$$\frac{Q_2}{Q_1} = \frac{D_2^3}{D_1^3}. \tag{C.6}$$

In other words, the zero-pressure and Murray-law methods are roughly equivalent if long flow extensions, with lengths proportional to the respective outlet diameters, are systematically added to the CFD model.

Notwithstanding the above, the assumption that both outlets have the same pressure is only valid if both daughter branches (or, in the general case, all outflow branches) somehow merge downstream, which is rarely the case. Instead, all arterial branches eventually terminate at some distal vascular bed. If we assume that the

2 daughter branches feed vascular beds of equal resistance, Equation C.1 becomes

C.7a) $$p_b - p_v = Q_1(R_1 + R_{bed})$$

C.7b) $$p_b - p_v = Q_2(R_2 + R_{bed}),$$

where $p_v$ is the pressure distal to the vascular bed (ie, the venous-side pressure) and $R_{bed}$ is the (downstream) vascular bed resistance, which is in series with the (upstream) daughter branch resistances. Equation C.7 obviously reduce to

C.8) $$\frac{Q_2}{Q_1} = \frac{R_1 + R_{bed}}{R_2 + R_{bed}},$$

and since vascular bed (ie, arteriolar and capillary) resistances are typically much greater than individual artery resistances, (ie, $R_{bed} \gg R_i$), Equation C.8 simplifies to

C.9) $$Q_1 \approx Q_2.$$

If one compares Equations C.4 and C.9, it should be clear that the equal (or zero) pressure outflow condition is different from the more physiological assumption of equal outflow resistances. With the addition of carefully tuned long outflow branches, however, the zero-pressure method might yield outflows comparable with those of the Murray-law method.

### *D) Splitting versus Murray's Law for a Multibranch Case*

Consider now the schematic diagram shown in On-line Fig 4, which represents the most common configuration of the 3D models in our cohort. The conventional Murray-law approach to estimating outflows is to apportion them on the basis of their relative diameters cubed. In this case, for example, the proportion of flow to, say, the M2b outlet would be

D.1) $$\frac{Q_{M2b}}{Q_{ICA}} = \frac{D^3_{M2b}}{\sum D^3_{outlet}} = \frac{D^3_{M2b}}{D^3_{A1} + D^3_{OA} + D^3_{M2a} + D^3_{M2b}},$$

and similarly for the other outlets. This requires no accounting for how the vessels branch within the model (ie, it depends only on the outlet diameters).

For our splitting method, on the other hand, we consider separately the power law outflow division (Equation B.1) at each bifurcation. For example, at the ICA/C7/OA branching, we have

D.2) $$\frac{Q_{C7}}{Q_{OA}} = \frac{D^n_{C7}}{D^n_{OA}},$$

where for now, we make no assumption about the value of the exponent, $n$. Owing to flow rate conservation (Equation B.2), Equation D.2 can be expressed equivalently as

D.3) $$\frac{Q_{C7}}{Q_{ICA} - Q_{C7}} = \frac{D^n_{C7}}{D^n_{OA}},$$

which, with re-arrangement of terms, becomes

D.4) $$\frac{Q_{C7}}{Q_{ICA}} = \frac{D^n_{C7}}{D^n_{OA} + D^n_{C7}}.$$

Similarly, for the C7/A1/M1 and M1/M2a/M2b branching, we obtain, respectively

D.5) $$\frac{Q_{M1}}{Q_{C7}} = \frac{D^n_{M1}}{D^n_{M1} + D^n_{A1}}$$

and

D.6) $$\frac{Q_{M2b}}{Q_{M1}} = \frac{D^n_{M2b}}{D^n_{M2a} + D^n_{M2b}}.$$

Multiplying Equations D.4, D.5, and D.6 together we obtain

D.7) $$\frac{Q_{M2b}}{Q_{ICA}} = \left(\frac{D^n_{C7}}{D^n_{C7} + D^n_{OA}}\right)\left(\frac{D^n_{M1}}{D^n_{M1} + D^n_{A1}}\right)\left(\frac{D^n_{M2b}}{D^n_{M2a} + D^n_{M2b}}\right).$$

It is therefore easy to see how, for the splitting method, the proportion of inflow to any outlet is simply the accumulated product of the respective upstream flow divisions.

So far, for the splitting method, for a given branching, we have assumed a power law relationship only for the daughter branches. If we were also to invoke the geometric power law relationship Equation B.3, Equation D.7 reduces to

D.8) $$\frac{Q_{M2b}}{Q_{ICA}} = \left(\frac{D^n_{C7}}{D^n_{ICA}}\right)\left(\frac{D^n_{M1}}{D^n_{C7}}\right)\left(\frac{D^n_{M2b}}{D^n_{M1}}\right).$$

If we now assume $n = 3$ for all bifurcations, this simplifies to

D.9) $$\frac{Q_{M2b}}{Q_{ICA}} = \frac{D^3_{M2b}}{D^3_{ICA}}.$$

Similarly, if we invoke Equation B.3 for the Murray-law method, Equation D.1 simplifies to

D.10) $$\frac{Q_{M2b}}{Q_{ICA}} = \frac{D^3_{M2b}}{D^3_{A1} + D^3_{OA} + D^3_{M1}} = \frac{D^3_{M2b}}{D^3_{C7} + D^3_{OA}} = \frac{D^3_{M2b}}{D^3_{ICA}}.$$

Thus, the Murray-law and splitting methods will give identical results if and only if the following: 1) Every branch internal to the model has the same power law exponent; and 2) the parent and daughter branches of each bifurcation follow a geometric power law (ie, Equation B.3). However, condition 1 likely does not hold for cerebrovascular models that include the ICA[4]; and condition 2 shows more interindividual scatter for the geometric power law than for the less restrictive flow ratio power law[3] (ie, Equation B.1).

## REFERENCES


1. Murray CD. **The physiological principle of minimum work, I: the vascular system and the cost of blood volume.** *Proc Natl Acad Sci U S A* 1926;12:207–14 CrossRef Medline
2. Zamir M, Sinclair P, Wonnacott TH. **Relation between diameter and flow in major branches of the arch of the aorta.** *J Biomech* 1992;25:1303–10 CrossRef Medline
3. Chnafa C, Bouillot P, Brina O, et al. **Vessel calibre and flow splitting relationships at the internal carotid artery terminal bifurcation.** *Physiol Meas* 2017;38:2044–57 CrossRef Medline
4. Ingebrigtsen T, Morgan MK, Faulder K, et al. **Bifurcation geometry and the presence of cerebral artery aneurysms.** *J Neurosurg* 2004;101:108–13 CrossRef Medline
5. Zarrinkoob L, Ambarki K, Wåhlin A, et al. **Blood flow distribution in cerebral arteries.** *J Cereb Blood Flow Metab* 2015;35:648–54 CrossRef Medline

6. MacDonald ME, Frayne R. **Phase contrast MR imaging measurements of blood flow in healthy human cerebral vessel segments.** *Physiol Meas* 2015;36:1517–27 CrossRef Medline
7. Wåhlin A, Ambarki K, Birgander R, et al. **Measuring pulsatile flow in cerebral arteries using 4D phase-contrast MR imaging.** *AJNR Am J Neuroradiol* 2013;34:1740–45 CrossRef Medline
8. Bammer R, Hope TA, Aksoy M, et al. **Time-resolved 3D quantitative flow MRI of the major intracranial vessels: initial experience and comparative evaluation at 1.5T and 3.0T in combination with parallel imaging.** *Magn Reson Med* 2007;57:127–40 CrossRef Medline
9. Enzmann DR, Ross MR, Marks MP, et al. **Blood flow in major cerebral arteries measured by phase-contrast cine MR.** *AJNR Am J Neuroradiol* 1994;15:123–29 Medline
10. Zhao M, Amin-Hanjani S, Ruland S, et al. **Regional cerebral blood flow using quantitative MR angiography.** *AJNR Am J Neuroradiol* 2007;28:1470–73 CrossRef Medline

**On-line Table 1: Enriched version of Table 1, showing predicted flow rates (mL/min) for various permutations of the outflow method and power law exponent**

| Outflow Method | ACA | MCA | OA | PcomA | ACA/MCA |
|---|---|---|---|---|---|
| No. of cases having artery | 67 | 70 | 52 | 12 | 67 |
| Zero-pressure | 103 ± 50 | 137 ± 53 | 15 ± 10 | 71 ± 42 | 43:57 |
| Murray-law ($n = 3$) | 89 ± 47 | 152 ± 57 | 14 ± 11 | 65 ± 46 | 37:63 |
| Murray-law ($n = 2$) | 81 ± 37 | 153 ± 51 | 22 ± 10 | 65 ± 35 | 34:66 |
| Splitting ($n = 3$) | 77 ± 42 | 174 ± 54 | 5 ± 4 | 45 ± 38 | 30:70 |
| Splitting ($n = 2$) | 86 ± 38 | 154 ± 46 | 16 ± 8 | 60 ± 30 | 36:64 |

**Note:**—$n$ = power law exponent.

**On-line Table 2: Literature values used to compute the weighted in vivo average shown in Table 1[a]**

| Literature Values | ACA | MCA | OA | PCA | ACA/MCA |
|---|---|---|---|---|---|
| Zarrinkoob et al[5] ($N = 94$) | 82 ± 18 | 146 ± 31 | 11 ± 5 | 54 ± 12 | 36:64 |
| MacDonald and Frayne[6] ($N = 30$) | 103 ± 41 | 142 ± 44 | – | 63 ± 24 | 42:58 |
| Wåhlin et al[7] ($N = 20$) | 87 ± 21 | 144 ± 32 | – | – | 38:62 |
| Bammer et al[8] ($N = 14$) | 59 ± 21 | 98 ± 32 | – | 49 ± 16 | 38:62 |
| Enzmann et al[9] ($N = 10$) | 82 ± 11 | 116 ± 8 | – | 52 ± 5 | 41:59 |
| Zhao et al[10] ($N = 83$) | 83 ± 27 | 148 ± 29 | – | 65 ± 14 | 36:64 |
| Weighted average | 84 ± 24 | 142 ± 31 | 11 ± 5 | 59 ± 14 | 37:63 |

**Note:**—$N$ indicates the number of cases in referenced article.

[a] References are from the On-line Appendix.

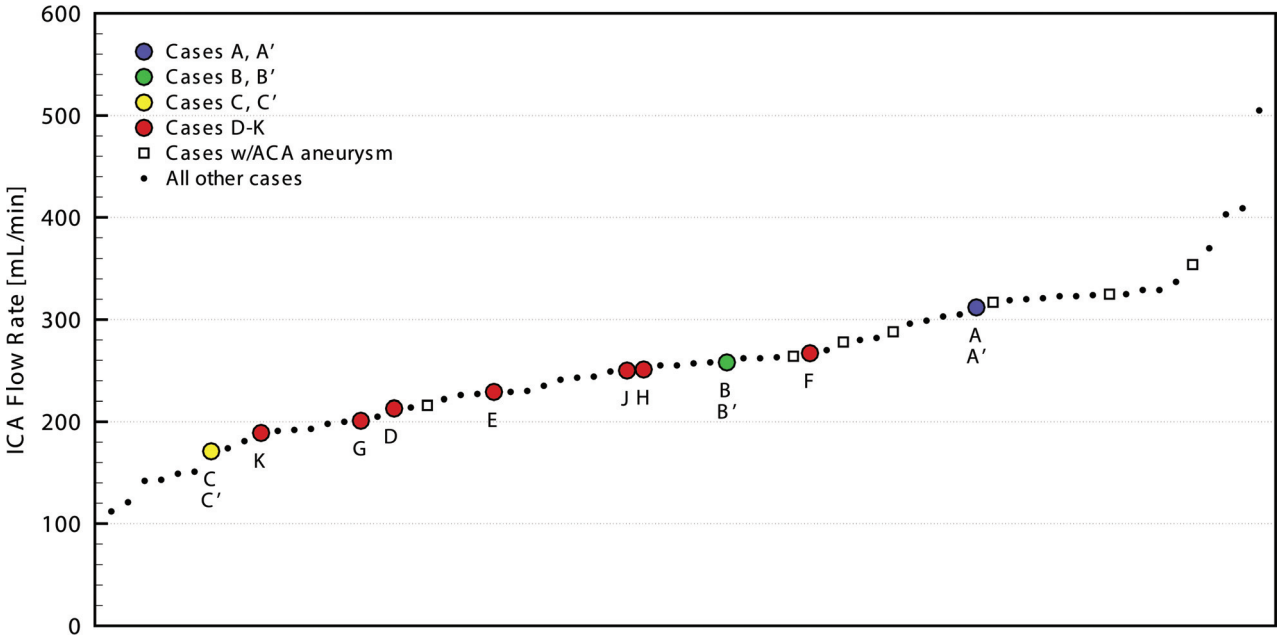


**ON-LINE FIG 1.** Flow rates imposed at the ICA inlet for the 70 cases of the study, ordered from lowest to highest. The flow rates are 257 ± 67 mL/min. Note the letters identifying the 10 3D CFD cases and their 3 variants, as shown in Fig 1.

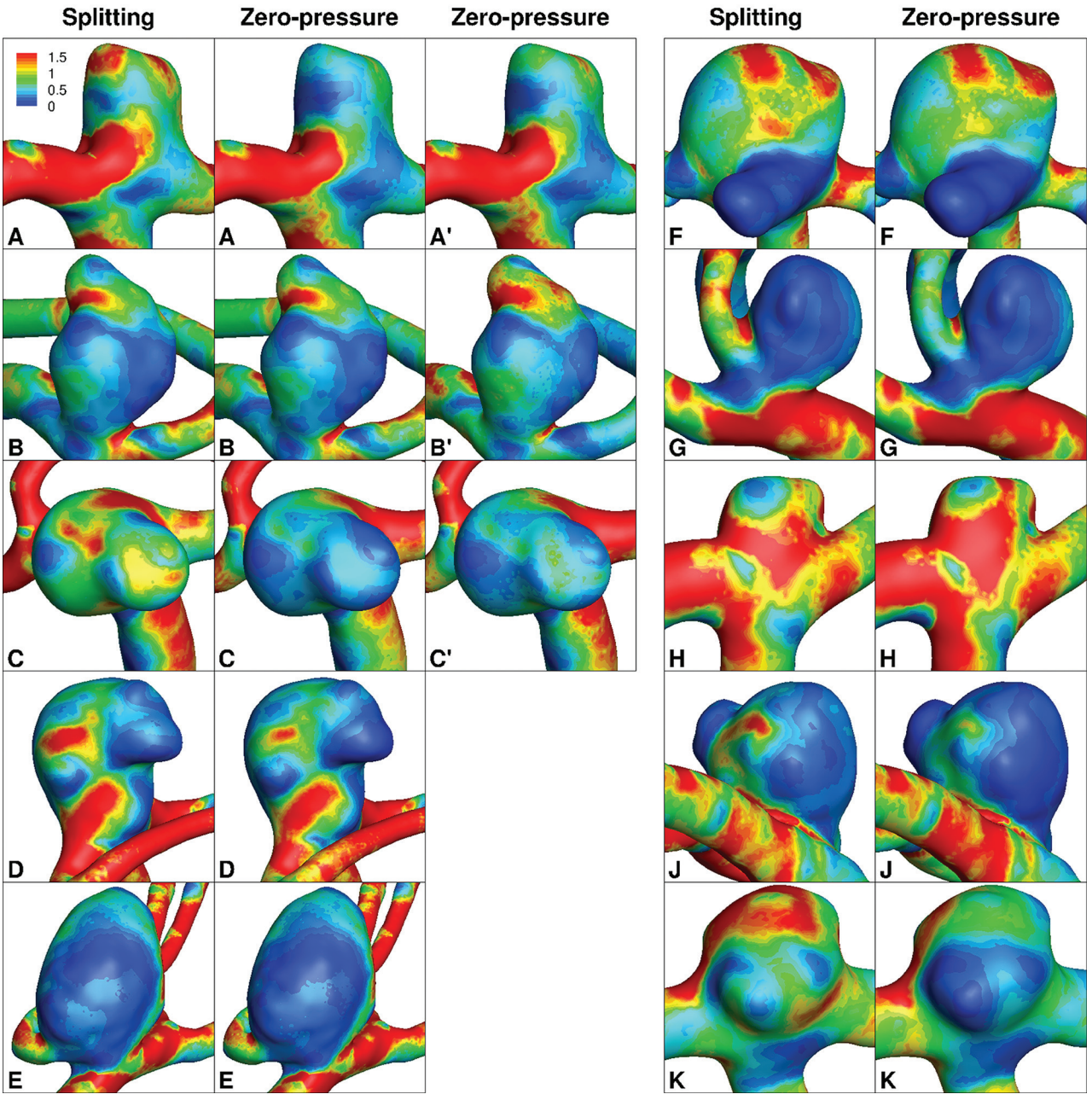


**ON-LINE FIG 2.** Surface distributions of TAWSS, normalized to the respective parent artery TAWSS, for the 10 3D CFD cases and their 3 variants.

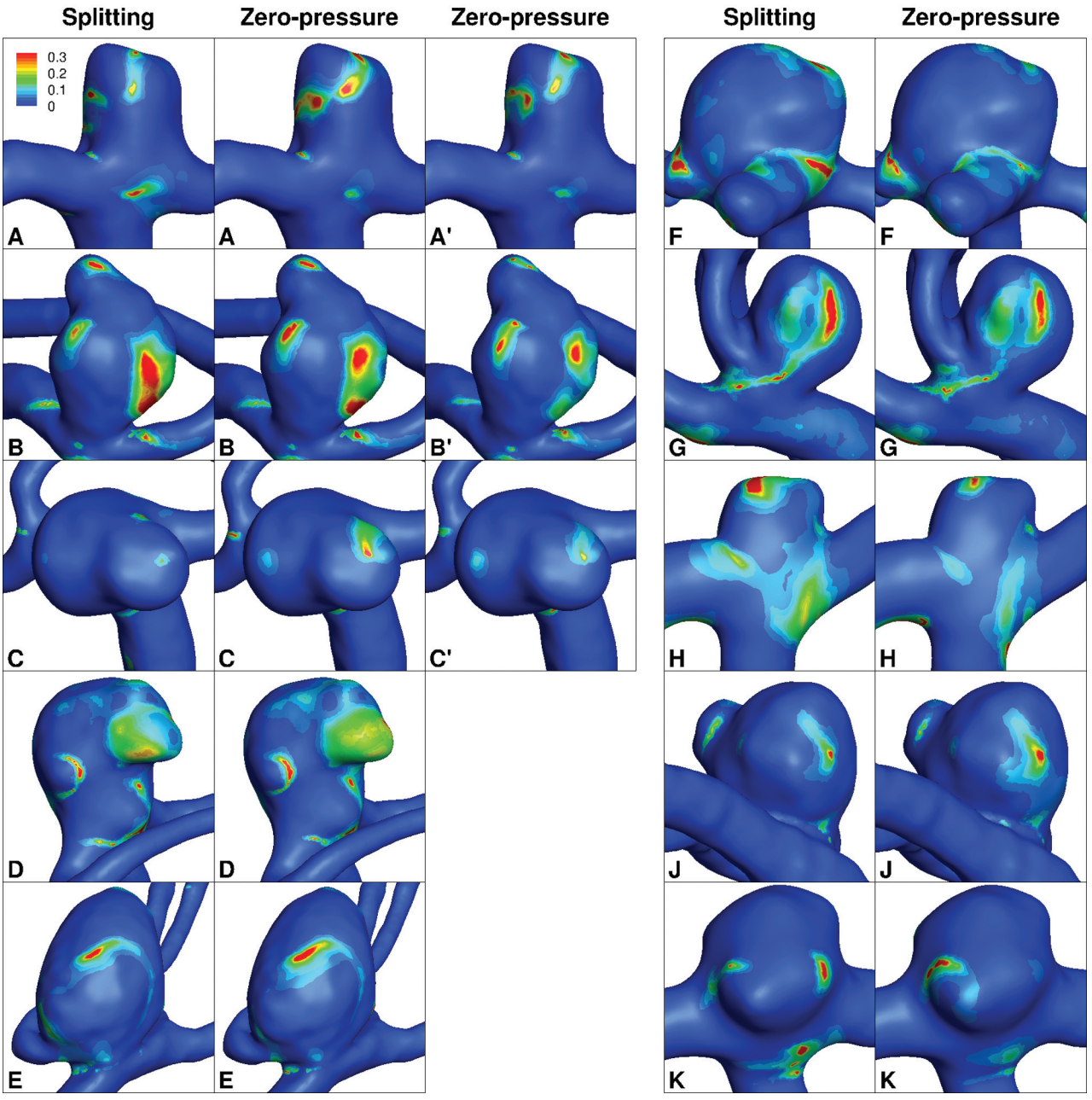


**ON-LINE FIG 3.** Surface distributions of OSI for the 10 3D CFD cases and their 3 variants.

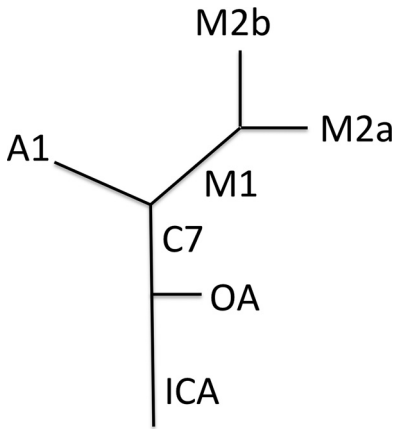


**ON-LINE FIG 4.** Schematic diagram of a typical branching in our cohort.